PHYSICAL REVIEW B **88**, 201103(R) (2013)

Kondo effect in monolayer and bilayer graphene: Physical realizations of the multichannel Kondo models

Maxim Kharitonov and Gabriel Kotliar
Center for Materials Theory, Rutgers University, Piscataway, New Jersey 08854, USA
(Received 30 April 2013; published 8 November 2013)

We perform a general group-theoretical study of the Kondo problem in monolayer and bilayer graphene around the charge neutrality point. Utilizing the group representation theory, we derive from symmetry considerations a family of the Kondo models for all symmetric placements with either a 3- or a 6-fold rotational axis of an impurity atom in an arbitrary orbital state. We find six possible classes of the partially anisotropic four-channel Kondo model. As the key result, we argue several possibilities to realize the regime of the dominant channel-symmetric two-channel Kondo effect, protected by the local symmetry and specifics of the graphene band structure. Our findings open prospects for the observation of the rich multichannel Kondo physics in graphene and the associated non-Fermi-liquid behavior.

DOI: 10.1103/PhysRevB.88.201103 PACS number(s): 72.80.Vp, 71.27.+a, 73.20.Hb, 75.30.Hx

Introduction and main results. The Kondo effect—the interaction of local spin or orbital degrees of freedom with conduction electrons—plays a fundamental role in a wide variety of condensed matter systems, ranging from quantum dots to strongly correlated materials.[1,2] The Kondo effect in graphene[3] has attracted significant interest[4–21,23–27] due to its peculiar electronic properties and potential for the realization of the multichannel Kondo effects. A number of theoretical studies of the quantum impurity problem have been undertaken for monolayer graphene (MLG),[4–22] and many fewer for bilayer graphene (BLG).[23] However, the analysis of possible Kondo models in graphene has not yet been performed in its full generality. In particular, the feasibility of the multichannel Kondo effect in graphene remained a debated question: both pro[4,16,19] and con[21] arguments have been put forward.

Motivated by these interesting questions, in this Rapid Communication, we perform a general group-theoretical study of the Kondo effect in MLG and Bernal-stacked BLG around the charge neutrality point (CNP). Following the original recipe of Nozieres and Blandin,[1] we utilize the group representation theory[28,29] to derive the family of four-channel Kondo models for all symmetric placements with either a 3- or a 6-fold rotational axis of an impurity atom (IA) in an arbitrary orbital state without appealing to any microscopic details. We find six possible classes of the Kondo models: there are three cases for the structure of conduction electron channels and the impurity can be in either a singlet or doublet orbital state.

Most importantly, we argue that in several cases of the impurity placement the two-channel Kondo effect is realized, where the exchange couplings for a pair of equivalent channels $E_e\pm$ belonging to one two-dimensional (2D) irreducible representation (IR) E_e are dominant. In these cases, in the low-energy regime, the symmetric two-channel Kondo model

$$\tilde{\hat{H}}_J^{\text{sglt}} = \hat{\psi}^\dagger_{E_e}(0)(J^{\rho E_e E_e} + J^{\sigma E_e E_e}\boldsymbol{\sigma}\mathbf{S})\hat{\psi}_{E_e}(0) \tag{1}$$

is realized in the orbital singlet case and the two-channel Kondo model

$$\tilde{\hat{H}}_J^{\text{dblt}} = \hat{\psi}^\dagger_{E_e}(0)\sum_{\gamma=0,x,y,z}\left(J_\gamma^{\rho E_e E_e} + J_\gamma^{\sigma E_e E_e}\boldsymbol{\sigma}\mathbf{S}\right)\tau_\gamma T_\gamma \hat{\psi}_{E_e}(0) \tag{2}$$

with partially anisotropic ($J_x^{\cdots} = J_y^{\cdots} \neq J_z^{\cdots}$) orbital Kondo interactions is realized in the orbital doublet case. Here, $\hat{\psi}_{E_e} = (\hat{\psi}_{E_e+\uparrow}, \hat{\psi}_{E_e+\downarrow}, \hat{\psi}_{E_e-\uparrow}, \hat{\psi}_{E_e-\downarrow})^t$ is a spinor in the product of the channel ($E_e\pm$) and spin ($\uparrow,\downarrow$) spaces, τ_γ and T_γ are unity ($\gamma = 0$) and Pauli ($\gamma = x,y,z$) matrices in the channel and impurity orbital doublet spaces, respectively, $\boldsymbol{\sigma} = (\sigma_x,\sigma_y,\sigma_z)$ are spin Pauli matrices of conduction electrons, and $\mathbf{S} = (S_x,S_y,S_z)$ are the impurity spin operators.

Both models present considerable physical interest, largely due to non-Fermi-liquid behavior exhibited in a number of regimes, but have proven challenging to realize in practice. Our findings thus pose MLG and BLG as promising materials for the realization of the rich multichannel Kondo physics and associated non-Fermi-liquid behavior.

Graphene lattice and local symmetry of the impurity atom. MLG and BLG[3] are two-dimensional carbon allotropes, shown in Fig. 1. Both have a triangular Bravais lattice with primitive translation vectors $\mathbf{a}_{1,2}$. MLG has $P6/mmm$ space group and D_{6h} point group; its unit cell contains two atoms denoted A and B. BLG has $P\bar{3}m1$ space group and D_{3d} point group; its unit cell contains four atoms A, B, $\tilde{A}$, and $\tilde{B}$, two in each layer.

In the presence of the IA, the spatial symmetry is reduced to a point group G,[28,29] with the center of the impurity being the fixed point. In this communication, we consider only such impurity placements that G contains either a 3- or 6-fold rotational axis (these, at the same time, may be the likely adsorption sites). Only in these cases (for a hexagonal lattice) G has 2D IRs, which is a necessary condition for the realization of the channel-symmetric 2-channel Kondo effect. Lower-symmetry point groups have no 2D IRs, in which cases the 2-channel Kondo effect is not feasible.

For MLG, there are two such vertical axes, denoted a and b (Fig. 1). For axis a going through the center of the carbon hexagon, $G = C_{6v}$, if the IA is out of the MLG mirror plane and $G = D_{6h} = C_{6v} \times C_s$ (C_s is the group of mirror reflection $z \leftrightarrow -z$), if the IA is in the mirror plane. For axis b going through the center of the carbon atom, $G = C_{3v}$, if the IA is out of the MLG plane, and $G = D_{3h} = C_{3v} \times C_s$, if the IA is in the MLG plane (i.e., IA substitutes the carbon atom).

For BLG, there also are two such vertical axes, denoted c and d (Fig. 1). For axis c going through the center of the

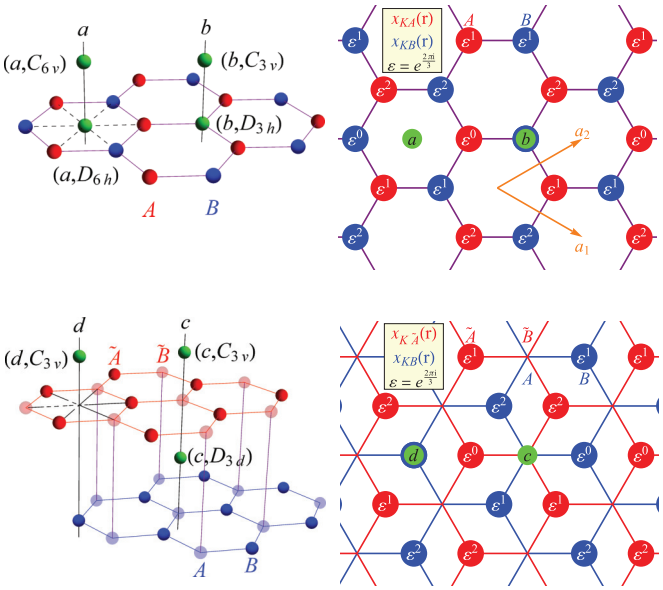

FIG. 1. (Color online) Lattice structure of MLG (top) and BLG (bottom) and considered IA placements (green). The phases $\varepsilon^{0,1,2}$, $\varepsilon = e^{2\pi i/3}$, of the Bloch wave functions $\chi_{KA,KB}(\mathbf{r})$ in MLG (top right) and $\chi_{K\tilde{A},KB}(\mathbf{r})$ in BLG (bottom right) are shown.

hexagon of one layer and a carbon atom (B) of the other layer, $G = C_{3v}$ for any of the vertical position of IA on the axis. For axis d going through two carbon atoms (A and $\tilde{B}$) of the layers, $G = D_{3d} = C_{3v} \times C_i$ (C_i is the point group of inversion), if the IA is at the midpoint between the layers, and $G = C_{3v}$ for any other IA placement on the axis. These cases are summarized in Table I.

Impurity degrees of freedom. A generalized Kondo model[1,2] describes minimal coupling of the conduction electrons to the spin and (if present) orbital degrees of freedom of a decoupled IA, i.e., neglecting the hybridization to the conduction states. The decoupled IA has a definite electron occupancy number N and spin S (according to the Hund's rule, $S = N/2$ and $S = 2l + 1 - N/2$ for less- and more-than-half-filled orbital with angular momentum l, respectively). In the crystalline environment, the orbital ground state of the IA belongs to one of the IRs R_i of G (we assume spin-orbit interactions weak). In all cases we consider (Table I), G has only 1D or 2D IRs.[28,29] Thus, the IA ground state is either an orbital *singlet* $|S_z\rangle$ or *doublet* $|\alpha\rangle \otimes |S_z\rangle$ if it belongs to one of the 1D ($R_i = A_i$) or 2D ($R_i = E_i$) IRs, respectively. Here, A_i and E_i denote *arbitrary* 1D and 2D IRs of the impurity orbital state, respectively, $S_z = -S, \ldots, S$, and $\alpha = \pm$ are the quantum

TABLE I. Considered cases of IA placement (first column), labeled by the rotational axis a,b,c,d and symmetry group G (Fig. 1) and decompositions of the 4D space R_e of conduction electrons into IRs of G (second column).

MLG	R_e
(a, C_{6v})	$E_1 + E_2$
(a, D_{6h})	$E_1'' + E_2''$
(b, C_{3v})	$A_1 + A_2 + E$
(b, D_{3h})	$A_1'' + A_2'' + E''$

BLG	R_e
(c, C_{3v})	$2E = E^{\alpha} + E^{\beta}$
(c, D_{3d})	$E_g + E_u$
(d, C_{3v})	$A_1 + A_2 + E$

numbers of the orbital doublet $R_i = E_i$. We choose the basis states $|\alpha = \pm\rangle$ so that they transform as $e^{\alpha i\varphi}$ under C_{3v} if $R_i = E$, and as $e^{\alpha i\varphi}$ and $e^{-\alpha 2i\varphi}$ under C_{6v} if $R_i = E_2, E_1$, respectively.

Thus, among the variety of microscopic possibilities of different l, N, and sequences of crystal field splittings, group theoretically, there are only two different classes of the orbital state of IA.

Conduction electron channels in MLG and BLG. The electronic band structure in both MLG and BLG[3,30,31] around zero doping is governed by four Bloch states $\chi_\mu(\mathbf{r})$ (Fig. 1), $\mu = KA, KB, K'A, K'B$ in MLG and $\mu = K\tilde{A}, KB, K'\tilde{A}, K'B$ in BLG, at two high-symmetry points referred to as valleys K and K', with energy $\epsilon = 0$ exactly at the charge neutrality point (CNP). The states in the two valleys are related by time-reversal symmetry: $\chi_{K'\ldots}(\mathbf{r}) = \chi^*_{K\ldots}(\mathbf{r})$. In MLG, the two states per valley reside on either A or B sublattice and are labeled accordingly. In BLG, the two states per valley reside on either $\tilde{A}$ or B sublattice, located in different layers, while their weight on the A and $\tilde{B}$ sublattices vanishes.

These four states $\chi_\mu(\mathbf{r})$ form 4D IRs of the respective space groups of MLG and BLG, which become reducible representations R_e of the impurity symmetry group G. Applying the symmetry operations of G to $\chi_\mu(\mathbf{r})$ in each considered case, we obtain the decomposition of R_e into IRs of G (Table I) and their basis functions $\chi_\eta(\mathbf{r})$ (Table I of the Supplemental Material;[32] η label the basis states of the IRs). Similarly to the impurity states $|\alpha = \pm\rangle$, we choose the basis states of the 2D IRs so that they transform as $\chi_{E\pm} \sim e^{\pm i\varphi}$ under C_{3v} and as $\chi_{E_2\pm} \sim e^{\pm i\varphi}$ and $\chi_{E_1\pm} \sim e^{\mp 2i\varphi}$ under C_{6v}. This convention eventually leads to the most natural form of orbital Kondo interactions (Table II).

We find that the seven considered cases of the impurity placement fall into 3 different classes, presented as columns of Table II: the conduction states R_e split into (I) two different 2D IRs; (II) one 2D and two 1D IRs; (III) two 2D IRs of the same type. For the cases (a,C_{6v}) and (b,C_{3v}) in MLG, our results for the classification of $\chi_\mu(\mathbf{r})$ agree with earlier results of Refs. 13,14,16.

The vicinity of CNP can be described by the low-energy expansion of the electron field operator

$$\hat{\Psi}_{\sigma=\uparrow,\downarrow}(\mathbf{r}) = \sum_\eta \chi_\eta(\mathbf{r})\hat{\psi}_{\eta\sigma}(\mathbf{r})$$

in terms of the exact eigenstates $\chi_\eta(\mathbf{r})$ at $\epsilon = 0$ and the operators $\hat{\psi}_{\eta\sigma}(\mathbf{r})$ that vary over large spatial scales. At such scales, the atomic impurity may be considered as a point object, whose degrees of freedom couple only to the conduction states with nonvanishing weight $\hat{\psi}_{\eta\sigma}(0)$ at its position $\mathbf{r} = 0$. As the solution for the single-particle spectrum in polar coordinates shows, see Refs. 4,16,19 and the Supplemental Material,[32] for both MLG and BLG there is exactly one such radial channel for each of the four components $\hat{\psi}_{\eta\sigma}(\mathbf{r})$ per σ. By the standard "unfolding" procedure,[2] where the outgoing and incoming radial waves are mapped to the plane waves in $s > 0$ and $s < 0$ regions of the effective 1D axis, these four channels can be represented as chiral 1D channels with kinetic energy

$$\hat{H}_0 = \int ds\, \hat{\psi}^\dagger(s)(-i\partial_s - \epsilon_F)\hat{\psi}(s). \qquad (3)$$

TABLE II. The most general forms allowed by symmetry of the exchange interaction Hamiltonian $\hat{H}_J$ [Eq. (4)] in MLG and BLG around the CNP for all possible IA placements with either a 3- or a 6-fold rotational axis (Fig. 1 and Table I). The entries are the expressions for $\hat{J}^{\rho,\sigma}$; both have identical structure in R_e but their own sets of coupling constants $J^{\rho\cdots}_{\cdots}$ and $J^{\sigma\cdots}_{\cdots}$; we suppress the indices ρ,σ for brevity. In (I), $E_{e1,e2} = E_{1,2}, E''_{1,2}, E_{g,u}$; in (II), $T_\pm = T_x \pm iT_y$. In the orbital doublet case, the summation goes over $\gamma = 0,x,y,z$ and everywhere $J^{\cdots}_x = J^{\cdots}_y$, since $\tau_x T_x + \tau_y T_y$ is an invariant.

$\hat{J}^{\rho,\sigma}$	(I) MLG: $(a, C_{6v}/D_{6h})$; BLG: (c, D_{3d})	(II) MLG: $(b, C_{3v}/D_{3h})$; BLG: (d, C_{3v})	(III) BLG: (c, C_{3v})
sglt.:	$\begin{pmatrix} J^{E_{e1}E_{e1}} & 0 \\ 0 & J^{E_{e2}E_{e2}} \end{pmatrix} \otimes \tau_0$	$\begin{pmatrix} J^{A_1A_1} & 0 & (0,0) \\ 0 & J^{A_2A_2} & (0,0) \\ (0,0)^t & (0,0)^t & J^{EE}\tau_0 \end{pmatrix}$	$\begin{pmatrix} J^{E^\alpha E^\alpha} & J^{E^\alpha E^\beta} \\ J^{E^\alpha E^\beta *} & J^{E^\beta E^\beta} \end{pmatrix} \otimes \tau_0$
dblt.:	$\sum_\gamma \begin{pmatrix} J_\gamma^{E_{e1}E_{e1}} & 0 \\ 0 & J_\gamma^{E_{e2}E_{e2}} \end{pmatrix} \otimes \tau_\gamma T_\gamma$	$\begin{pmatrix} J^{A_1A_1}T_0 & J^{A_1A_2}T_z & J^{A_1E}(T_-, T_+) \\ \text{H.c.} & J^{A_2A_2}T_0 & J^{A_2E}(T_-, -T_+) \\ \text{H.c.} & \text{H.c.} & \sum_\gamma J_\gamma^{EE}\tau_\gamma T_\gamma \end{pmatrix}$	$\sum_\gamma \begin{pmatrix} J_\gamma^{E^\alpha E^\alpha} & J_\gamma^{E^\alpha E^\beta} \\ J_\gamma^{E^\alpha E^\beta *} & J_\gamma^{E^\beta E^\beta} \end{pmatrix} \otimes \tau_\gamma T_\gamma$
	$\hat{\psi} = (\hat{\psi}_{E_{e1}+}, \hat{\psi}_{E_{e1}-}, \hat{\psi}_{E_{e2}+}, \hat{\psi}_{E_{e2}-})^t$	$\hat{\psi} = (\hat{\psi}_{A_1}, \hat{\psi}_{A_2}, \hat{\psi}_{E+}, \hat{\psi}_{E-})^t$	$\hat{\psi} = (\hat{\psi}_{E^\alpha+}, \hat{\psi}_{E^\alpha-}, \hat{\psi}_{E^\beta+}, \hat{\psi}_{E^\beta-})^t$

We arrange the operators $\hat{\psi}_{\eta\sigma}$ into eight-component spinors $\hat{\psi}$ presented in Table II, where $\hat{\psi}_\eta = (\hat{\psi}_{\eta\uparrow}, \hat{\psi}_{\eta\downarrow})^t$. Thus, for an atomic-size impurity, a 4-channel Kondo model is generically realized in MLG[4,16,19] and BLG around CNP.

Kondo models from the symmetry approach. We now derive the Kondo models. As first outlined by Nozieres and Blandin[1] and later implemented in a number of works for various Kondo systems,[2,33] the most general possible form of the exchange interaction Hamiltonian $\hat{H}_J$ can be obtained based on the symmetry grounds without appealing to any microscopic model: $\hat{H}_J$ must remain invariant under all symmetry operations of the system. The most general form invariant under spin rotations reads

$$\hat{H}_J = \hat{\psi}^\dagger(0)(\hat{J}^\rho + \hat{J}^\sigma \boldsymbol{\sigma}\mathbf{S})\hat{\psi}(0). \tag{4}$$

In Eq. (4), $\hat{J}^{\rho,\sigma}$ are the operators in the orbital sector $R_e \otimes R_i$: they are 4×4 matrices in the orbital space R_e of conduction electrons; in the impurity doublet case, they also contain the orbital "isospin" operators T_γ, $\gamma = 0,x,y,z$ (unity and Pauli matrices) acting in the space $R_i = E_i$ of the states $|\alpha = \pm\rangle$.

The operators $\hat{J}^{\rho,\sigma}$ must remain invariant under the orbital symmetry group G.[34] Such invariant form is efficiently constructed using the algebra of the group representation theory[28,29] as follows.[1,2] The operators

$$\hat{J}^{\rho,\sigma} \sim (R_e \times R_e^\dagger) \times (R_i \times R_i^\dagger) \tag{5}$$

transform as a product of four representations of G, where $R_e \times R_e^\dagger$ and $R_i \times R_i^\dagger$ describe the transformation properties in the conduction electron and impurity subspaces, respectively. The decomposition of the product (5) into IRs can readily be calculated.[28,29] The only allowed terms in $\hat{J}^{\rho,\sigma}$ are the invariants, which transform according to the unity IR $A_1/A_1'/A_{1g}$ of G; each invariant may enter $\hat{J}^{\rho,\sigma}$ with its own coupling constant J. The explicit form of these invariants is constructed by utilizing the transformation properties of $\psi_{\eta\sigma}$ and $|\alpha = \pm\rangle$ under G.

This procedure yields the most general forms allowed by symmetry of the Kondo exchange interaction Hamiltonians $\hat{H}_J$ [Eq. (4)], presented in Table II; details of the derivation are provided in the Supplemental Material.[32] The contents of Table II, along with Table I and Eqs. (3) and (4), constitute the central result of our work. They describe the family of the four-channel Kondo models

$$\hat{H} = \hat{H}_0 + \hat{H}_J$$

in MLG and BLG in the vicinity of CNP for all possible seven cases (Table I) of the symmetric placements of the IA with either 3- or 6-fold rotational axis. In the rest of this communication, we discuss their key properties and physical implications.

Main properties. We find 6 possible classes of the Kondo models: there are the 3 above-mentioned classes (I), (II), and (III) (columns of Table II) for conduction electron states and two classes of impurity orbital states, singlet (sglt., $R_i = A_i$) and doublet (dblt., $R_i = E_i$) (rows of Table II). All cases of the impurity placement within one class have identical structure of the Kondo model.

In the orbital-singlet class (I) and (II) models, when conduction states R_e break into IRs of different types, the channels are not coupled by exchange interaction and the two channels belonging to the same 2D IR are characterized by the same coupling constant, protected by symmetry. These are prerequisites for the realization of the two-channel Kondo effect. On the other hand, in the orbital-singlet class (III) model, the conduction sea $R_e = 2E = E^\alpha + E^\beta$ consists of two 2D IRs of the same type E (the labels α,β are used to distinguish between the two subspaces). As a result the "conversion" processes $E^\alpha \leftrightarrow E^\beta$, whereby the conduction electrons are transferred between two IRs, are present.

In the orbital doublet case, for any class (I), (II), or (III), the two channels belonging to each 2D IR E_e couple to the impurity via anisotropic orbital Kondo interaction $J_0^{\cdots}\tau_0 T_0 + J_z^{\cdots}\tau_z T_z + J_\perp^{\cdots}(\tau_x T_x + \tau_y T_y)$, where τ_γ are unity ($\gamma = 0$) and Pauli ($\gamma = x,y,z$) matrices acting in the space of $E_e\pm$ states. The class (I) model consist of two decoupled two-channel contributions of this kind and there are no conversion processes $E_{e1} \leftrightarrow E_{e2}$ between them. In the class (II) model the conversion processes $A_1 \leftrightarrow A_2$ and $A_{1,2} \leftrightarrow E$ between all IRs are present. In class (III), the conversion processes $E^\alpha \leftrightarrow E^\beta$ between two 2D IRs of the same type are present as well, with the structure of the orbital Kondo interactions above.

Thus, our group-theoretical analysis allows us to make definitive symmetry-based conclusions about the structure of the Kondo model without relying on any specific microscopic details. In particular, it tells exactly whether and how different

conduction channels are coupled by the exchange interaction, Table II. We emphasize that generally the channel states $\chi_\eta(\mathbf{r})$ can be either pure valley states or mixtures thereof, as seen from Table I of the Supplemental Material.[32] This analysis also resolves the concern[21] that "valley mixing" by the impurity potential could be detrimental for the multichannel Kondo effect: while valleys can indeed be mixed, the local symmetry dictates that properly hybridized valley states act as independent channels in several instances (Table II), which are also completely equivalent if they belong to one 2D IR.

Feasibility of the channel-symmetric two-channel Kondo effect. We now discuss the implications of our results for the realization of the multichannel Kondo effects. It is well established[1,2] that the low-energy behavior of the multichannel Kondo model is determined by the channel(s) with the largest exchange coupling. Thus, effectively, the regime of the multichannel Kondo effect can be realized only if the common coupling of several channels (belonging to the same multidimensional IR) exceeds all single-channel couplings. This condition proved to be extremely hard to achieve in practice: in a "typical" band structure with no special properties, some single-channel coupling will usually prevail.

Our findings suggest that, owing to the peculiarities of graphene band structure, the regime of the dominant two-channel Kondo effect is feasible in MLG and BLG in several cases.

The class (I) Kondo model, which includes the cases $(a, C_{6v}/D_{6h})$ in MLG and (c, D_{3d}) in BLG, consists of two decoupled symmetric two-channel contributions with their own couplings. Whichever couplings are greater, the low-energy behavior will be dominated by the two channels of that 2D IR.

In the BLG (d, C_{3v}) case, if the IA is placed above the center of the carbon hexagon of one layer, as shown in Fig. 1, the atomic orbitals of the 2D IR E channels, located on the $\tilde{A}$ sublattice in that nearby layer, are much closer to the impurity than those of the 1D IR $A_{1,2}$ channels, located on the B sublattice in the remote layer. Thus the hybridization with the E channels is likely to be considerably greater than with $A_{1,2}$ channels. This should result in greater exchange couplings $J^{EE}_{\dots} > J^{A_{1,2}A_{1,2}}_{\dots}$ and the low-energy behavior will be dominated by the two E channels.

In these cases, in the low-energy regime, the symmetric two-channel Kondo models (1) and (2) will be realized in the orbital singlet and doublet cases, respectively, in the subspace of the two dominant channels $E_e\pm$.

Conclusion and outlook. In summary, motivated by the prospect of realizing multichannel Kondo effects, we performed a general group-theoretical classification of the Kondo models in MLG and BLG in the vicinity of the CNP for all placements of the IA with either 3- or 6-fold rotational symmetry. We found six possible classes of the four-channel Kondo models, summarized in Table II. We argued several possibilities for realizing the channel-symmetric two-channel Kondo effect, described by the models (1) and (2), which are known to exhibit non-Fermi-liquid behavior in a number of regimes but have proven challenging to realize in practice. When combined with *ab initio* simulations, such as those of Refs. 13,14,18, our results should enable one to make definitive conclusions not only about the possible forms of the low-energy Kondo models but also about the values of the exchange couplings realized for specific magnetic adatoms. Our findings thus open prospects for the observation of the multichannel Kondo physics in MLG and BLG, which could be pursued experimentally using the local probes, such as scanning tunneling microscopy, or transport measurements.

Acknowledgments. This work was supported by the US DOE under contract No. DE-FG02-99ER45790 and by NSF Grant No. DMR-0906943.

[1] Ph. Nozieres and A. Blandin, J. Phys. **41**, 193 (1980).
[2] D. L. Cox and A. Zawadowski, Adv. Phys. **47**, 599 (1998).
[3] A. H. Castro Neto, F. Guinea, N. M. R. Peres, K. S. Novoselov, and A. K. Geim, Rev. Mod. Phys. **81**, 109 (2009).
[4] K. Sengupta and G. Baskaran, Phys. Rev. B **77**, 045417 (2008).
[5] M. Hentschel and F. Guinea, Phys. Rev. B **76**, 115407 (2007).
[6] B. Dóra and P. Thalmeier, Phys. Rev. B **76**, 115435 (2007).
[7] P. S. Cornaglia, G. Usaj, and C. A. Balseiro, Phys. Rev. Lett. **102**, 046801 (2009).
[8] B. Uchoa, V. N. Kotov, N. M. R. Peres, and A. H. Castro Neto, Phys. Rev. Lett. **101**, 026805 (2008).
[9] B. Uchoa, L. Yang, S.-W. Tsai, N. M. R. Peres, and A. H. Castro Neto, Phys. Rev. Lett. **103**, 206804 (2009).
[10] B. Uchoa, T. G. Rappoport, and A. H. Castro Neto, Phys. Rev. Lett. **106**, 016801 (2011).
[11] B. Uchoa, L. Yang, S.-W. Tsai, N. M. R. Peres, and A. H. Castro Neto, arXiv:1105.4893.
[12] H.-B. Zhuang, Q.-F. Sun, and X. C. Xie, Eur. Phys. Lett. **86**, 58004 (2009).
[13] T. O. Wehling, H. P. Dahal, A. I. Lichtenstein, M. I. Katsnelson, H. C. Manoharan, and A. V. Balatsky, Phys. Rev. B **81**, 085413 (2010).
[14] T. O. Wehling, A. V. Balatsky, M. I. Katsnelson, A. I. Lichtenstein, and A. Rosch, Phys. Rev. B **81**, 115427 (2010).
[15] M. Vojta, L. Fritz, and R. Bulla, Europhys. Lett. **90**, 27006 (2010).
[16] Z.-G. Zhu, K.-H. Ding, and J. Berakdar, Europhys. Lett. **90**, 67001 (2010).
[17] Z.-G. Zhu and J. Berakdar, Phys. Rev. B **84**, 165105 (2011).
[18] D. Jacob and G. Kotliar, Phys. Rev. B **82**, 085423 (2010).
[19] L. Dell'Anna, J. Stat. Mech. (2010) P01007.
[20] M. A. Cazalilla, A. Iucci, F. Guinea, and A. H. Castro Neto, arXiv:1207.3135.
[21] L. Fritz and M. Vojta, Rep. Prog. Phys. **76**, 032501 (2013).
[22] C. R. Cassanello and E. Fradkin, Phys. Rev. B **53**, 15079 (1996); **56**, 11246 (1997).
[23] S. Lipinski and D. Krychowski, J. Korean Phys. Soc. **62**, 1440 (2013).
[24] J.-H. Chen, W. G. Cullen, E. D. Williams, and M. S. Fuhrer, Nat. Phys. **7**, 535 (2011).

[25] V. W. Brar, R. Decker, H.-M. Solowan, Y. Wang, L. Maserati, K. T. Chan, H. Lee, C. O. Girit, A. Zettl, S. G. Louie, M. L. Cohen, and M. F. Crommie, Nat. Phys. **7**, 43 (2011).

[26] J. Mao, I. Skachko, G. Li, and E. Andrei, http://meetings.aps.org/Meeting/MAR13/Event/188650

[27] T. Eelbo, M. Wasniowska, P. Thakur, M. Gyamfi, B. Sachs, T. O. Wehling, S. Forti, U. Starke, C. Tieg, A. I. Lichtenstein, and R. Wiesendanger, Phys. Rev. Lett. **110**, 136804 (2013).

[28] M. Hamermesh, *Group Theory and Its Application to Physical Problems* (Addison-Wesley, Reading, MA, 1962).

[29] L. D. Landau and E. M. Lifshitz, *Quantum Mechanics*, A Course of Theoretical Physics Vol. 3 (Pergamon Press, Oxford, 1965).

[30] P. R. Wallace, Phys. Rev. **71**, 622 (1947).

[31] E. McCann and V. I. Falko, Phys. Rev. Lett. **96**, 086805 (2006).

[32] See Supplemental Material at http://link.aps.org/supplemental/10.1103/PhysRevB.88.201103 for details.

[33] A. I. Toth and G. Kotliar, Phys. Rev. Lett. **107**, 266405 (2011).

[34] $\hat{H}_J$ must also remain invariant under the time reversal; we find, however, that the time-reversal symmetry does not impose any additional constraints.